Paulina PIANKO-OPRYCH, Ekaterina KASILOVA, Zdzisław JAWORSKI

e-mail: paulina.pianko@zut.edu.pl

**Zakład Projektowania Systemów i Optymalizacji Procesowej, Wydział Technologii i Inżynierii Chemicznej,
Zachodniopomorski Uniwersytet Technologiczny, Szczecin**

Modelling of processes in a microtubular Solid Oxide Fuel Cell

Introduction

Microtubular Solid Oxide Fuel Cells (mSOFC) are promising technology that allows to produce electricity in miniature portable devices [*Howe et al., 2011a,b*]. Quantitative analysis and interpretation of the conditions of high temperature fuel cells in real systems is difficult, time consuming and very expensive due to the required experimental access to fuel cells as well as to an appropriate laboratory infrastructure. Useful tools in that assessment are numerical codes of Computational Fluid Dynamics (CFD). CFD codes allow for a quantitative description of non-linear relationships between time varying parameters such as temperature, pressure, substrate and product streams. Complexity of the processes in fuel cells makes mathematical modelling of microtubular Solid Oxide Fuel Cells a very challengeable task, which requires a step-wise approach.

Since the end of the 1990s the method of Computational Fluid Dynamics (CFD) has been widely used to simulate the hydrodynamics, heat transfer as well as the charge and mass transfer in the SOFC [*Ferguson et al., 1996; Bistolfi et al., 1996*]. The main part of research efforts in the field of mSOFC has focused on the single mSOFC [*Cui et al., 2009; Akhtar et al. 2010; Kendall, 2010; Garcia-Camprubi et al., 2011; Amiri et al., 2013*]. The CFD models of mSOFC stacks were rather rare. It may be explained by the fact that configuration of mSOFCs in the stack has a synergetic effect on the complexity of the physical problem which is quite challengeable even for a single SOFC. The 3D simulations of hydrodynamics in the mSOFC stack consisting of 6 cells was presented by [*Lee et al., 2010*] using an User Defined Function subroutine implemented into the Fluent code. A simplified cell model was built to take into account an electrochemical reaction. Sets of the governing equations for momentum, energy and the species transport were simultaneously solved giving local profiles of temperatures, electrical current density and concentrations in the computational domain. The final purpose of the model was to design fuel manifold giving an uniform distribution of hydrogen concentration in the fuel channels of the single SOFC. No data relating to the simulation results for the SOFC voltage-current curves was reported [*Lee et al., 2010*].

Lee and Hong [*2010*] reported results for a micro-planar SOFC stack with 5 cells. The model was established by using a commercial CFD code ADINA. The numerical code was based on the standard Navier–Stokes equations and multi-dimensional predictions of the velocity, pressure, temperature and concentration fields were obtained. The electrochemistry end current distribution calculations were based on the *Butler-Volmer* equation [*Lee and Hong, 2010*]. The model was verified using experimental data of the authors for a small-sized stack.

Akhtar [*2012*] presented a comprehensive CFD model of the microtubular single-chamber SOFC stack. The model accurately took into account coupled processes such as heat, charge and mass transfer in the stack including also the chemical reactions, which were typical for the single-chamber configuration. The main restriction of the *Akhtar's* model was that it assumed only three cells in the stack since a higher number of cells resulted in a dramatic increase in the complexity of simulations. The model can be applied only to rather small laboratory-scale stacks and it is not suitable for industrial stacks having some dozens of mSOFCs.

The geometry of a microtubular SOFC stack containing 20 cells used by *Lockett et al.* [*2004*] was close to an industrial stack design. The whole test rig was defined as the computational domain. The main purpose of the model was to estimate temperature gradients in the cells. A serious disadvantage of the model was that the species and charge transport were not taken into account by the model.

It follows from the literature review that the detailed CFD models of the mSOFC stacks contain rather small number of cells or are based on simplified assumptions. At the same time, the system models often do not take into account hydrodynamics in SOFC at all [*Ameri and Mohammadi, 2011; Zhang et al., 2005*], which may be a serious restriction of predictive capability of the system model.

The method of modelling

The aim of this work was to establish a CFD model of the microtubular SOFC which could be used in system simulations. The model has to be able to predict the mSOFC performance by accounting for coupled processes of mass and charge transfer as well as hydrodynamics in the fuel cell. However, it has to be simple enough to be applicable in the modeling of mSOFC stacks containing a number of single fuel cells.

Therefore, a microtubular SOFC with supporting anode was adopted for simulations. The basic dimensions of the fuel cell is shown in Figure 1. The *COMSOL Multiphysics 4.3* [*2013*] was used in the simulations. The boundary conditions were defined in the code according to an experimental setup [*Howe and Kendall, 2011*]. During the experimental tests the mSOFC was placed into a furnace of the volume much larger than the SOFC volume. The fuel was pure hydrogen supplied to the gas channel. The furnace temperature was kept constant during test. The CFD model included experimental conditions presented in Tab. 1 [*Howe and Kendall, 2011*].
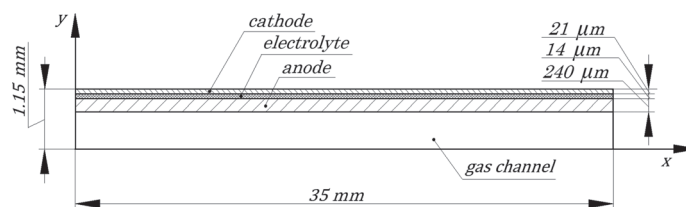

Fig. 1. Geometry of the mSOFC (not to scale) [*Howe and Kendall, 2011*]

Tab. 1. Simulation input data [*Howe and Kendall, 2011*]

Fuel	Fuel flow rate, [cm^3/s*]	Furnace (air) temperature, [^{o}C]	SOFC temperature, [^{o}C]	Open circuit voltage, [V]
H$_2$ high purity 99.95	20	650	750	1.1

* at the normal conditions

All layers of the SOFC membrane-electrode assembly including the thin cathode and electrolyte domains were resolved in the model. A non-uniform mesh was built in the COMSOL mesh generator with structured domains in the gas channel, electrolyte and cathode. The 2D triangular mesh was generated in the anode area with a set distribution of the element sizes to smooth the transition from the coarse mesh to the fine one in the gas channel and the electrolyte-cathode region, respectively. The average grid element quality was 0.98.

The case was numerically solved using the following assumptions:
- laminar flow in the fuel channel was applied due to low values of the fuel velocity and channel diameter with the *Reynolds* number value of the order of unity,
- a 2D model was adopted because of the axial symmetry of the cell geometry**.**
- the isothermal case was assumed. The SOFC temperature at the inlet to the fuel cell was 750°C according to the experimental data.

The mass conservation equation (1) was applied for porous flows:

$$\frac{\partial(\rho\varepsilon)}{\partial t} + \nabla \cdot (\rho\bar{u}) = Q_m \tag{1}$$

combined with the momentum balance equation. The porosity, ε, of 1 was assumed for the fuel channel.

The following forms of the momentum conservation equation were used for different regions of the computational domain. The fuel channel was described by the *Navier-Stokes* equations for laminar flows:

$$\rho\frac{\partial\bar{u}}{\partial t} + \rho(\bar{u}\cdot\nabla)\bar{u} = \nabla\cdot[-p\bar{I} + \mu[\nabla\bar{u} + (\nabla\bar{u})^T]] + F \tag{2}$$

However, the simplest *Darcy* approach was applied for the flow in the porous cathode of permeability, κ:

$$\bar{u} = -\frac{\kappa}{\mu}\nabla p \tag{3}$$

The *Brinkman* equation (4) was used for the anode to properly represent coupling of the fluid flow in the porous anode and in the gas channel [*Nield and Bejan, 2006*].

$$\frac{\rho}{\varepsilon}\left(\frac{\partial\bar{u}}{\partial t} + (\bar{u}\cdot\nabla)\frac{\bar{u}}{\varepsilon}\right) = \nabla\left[\frac{1}{3}\left\{\mu(\nabla\bar{u} + (\nabla\bar{u})^T) - \frac{2}{3}\mu(\nabla\cdot\bar{u})\bar{I}\right\}\right] +$$
$$+ \bar{F} - \nabla p - \left(\frac{\mu}{\kappa} + Q_m\right)\bar{u} \tag{4}$$

Mass transport of species i in the channel and the electrodes was described by the *Fick's* law:

$$\bar{j}_i = -M_i D_i \nabla c_i \tag{5}$$

and combined with the species conservation equation:

$$\frac{\partial}{\partial t}(\rho\omega_i) + \nabla\cdot(\rho\omega_i\bar{u}) = -\nabla\cdot\bar{j}_i + R_i \tag{6}$$

The connection between the mass fraction ω_i and the molar concentration c_i is given by equation:

$$\omega_i = \frac{M_i c_i}{\rho} \tag{7}$$

The effective diffusivity values (8) were used for the porous media simulated:

$$D_i^{eff} = \frac{\varepsilon}{\tau}D_i \tag{8}$$

where τ [-] is the tortuosity of the electrode pores.

The electrical submodel included the charge conservation equation:

$$\nabla\cdot i_k = Q_k \tag{9}$$

and the *Ohm's* law:

$$i_k = -\sigma_k\nabla\phi_k \tag{10}$$

The two equations of the electric submodel were solved for the electrolyte domain as well as for both the ionic conductive phase and the electronic conductive one in the two electrodes. The charge transfer processes in the anode and cathode were represented in the simulation as distributed species sources.

A binary H_2-H_2O fuel mixture was considered. No volumetric chemical reaction was assumed. Therefore the rate R_i of production or consumption of i-th component in both the anode and the cathode zones is determined by electrochemical reaction only and may be calculated according to the Faraday equation

$$R_i = M_i\frac{v_{i,m}i}{n_m F} \tag{11}$$

where i is the local current density value at the three-phase boundary. The activation polarization for the anode was calculated using the full formulation of the *Butler-Volmer* equation for a single-electron reaction:

$$i = i_0\left(\frac{c_i}{c_i^{ref}}\right)\left\{\exp\left(\frac{\alpha_a F\eta}{RT}\right) - \exp\left(-\frac{\alpha_c F\eta}{RT}\right)\right\} \tag{12}$$

where i is the current density [A/m^2], i_0 is the exchange current density [A/m^2], c_i is the actual concentration of the i-th component (H_2, H_2O) [mol/m^3], $c_{H_2}^{ref}$ and $c_{H_2O}^{ref}$ is the reference concentration of the i-th component [mol/m^3], γ_i is the concentration exponent for the i-th component

[-], α_a and α_c are the charge transfer coefficients [-], F is the *Faraday* number [C/mol], η is the activation polarization [V], R is the universal gas constant [J/molK], T is the temperature [K].

Boundary conditions for the simulation were set as follows:
– inlet of the fuel channel: velocity of 0.3 [m/s]; H_2 mass concentration of 90 [%], H_2O mass concentration of 10 [%],
– outlet of the fuel channel: pressure of 10^5 [Pa],
– outer boundary of the cathode: N_2 mass concentration of 79 [%], O_2 mass concentration of 21 [%], pressure of 10^5 [Pa],
– bottom boundary of the domain: symmetry,
– side boundary: no flux of any of the species.

Current collectors were supposed to be of ideally uniform mesh with conductivity much higher than the conductivity of the membrane-electrode assembly. Constant electrical potential values were set on the inner surface of the anode and outer surface of the cathode. The anode surface was assumed to be grounded, the electric potential of the cathode surface was varied in the range of 0.25÷1.1 [V] to result in the SOFC voltage-current curve.

There were no concentration limitations imposed on the current-voltage characteristic, which means that the SOFC performance was determined mainly by the ohmic and activation polarizations. The concentration polarization was not taken into account in the considered case. A constant equilibrium potential of the electrochemical reaction was set equal to 1.1 [V] according to the experimental value (Tab. 1).

The mass transfer process in the furnace was assumed to be intensive enough, therefore the gas composition on the outer side of the cathode was identical to the standard air composition.

The concentration exponents were assumed to be 1.0 for H_2 and 0.0 for H_2O similarly to the approach presented by *Kulikovsky* [*2009*]. Changing of the O_2 concentration along the cathode-electrolyte boundary surface caused an insignificant current variation along the SOFC length. Therefore, no concentration dependence of the cathode activation polarization was taken into account.

Tab. 2. Physical and electrochemical parameters for the MEA structure used in the simulation

Parameter	Value	Units
Porosity	0.3	-
Tortuosity	3	-
Permeability	10^{-14}	m^2
Electrolyte conductivity	1.4	Sm/m
Effective anode electronic conductivity	0.2	Sm/m
Effective anode ionic conductivity	10^5	Sm/m
Effective cathode electronic conductivity	0.2	Sm/m
Effective cathode ionic conductivity	10^3	Sm/m
Anode active surface area per volume	9·10^4	m^2/m^3
Cathode active surface area per volume	10^6	m^2/m^3
Anode exchange current density	2500	A/m^2
Cathode exchange current density	910	A/m^2

The structure and electrical properties of the SOFC Membrane-Electrode Assembly (MEA) were set according to the reference data [*Zeng et al., 2012; Costamagna et al., 1998; Hussain et al., 2009*]. The exchange current density values were treated as fit parameters (Table 2).

Results and discussion

Comparisons of the calculated voltage vs. power curves with the experimental results are presented in Fig. 2. The CFD curves correspond well to the experimental ones. The simulated fuel utilization value of 0.348 [-] at the peak power matched well the experimental estimate of 36 [%] [*Howe and Kendall, 2011*].

The simulated current distribution along the anode surface for varied cell voltage is presented in Fig. 3. The current value changes no more than 20 [%] along the mSOFC. That fact partly justifies the isothermal approach used in the model. An accurate representation of the heat transfer and concentration polarization in the cell will be a subject of further work.
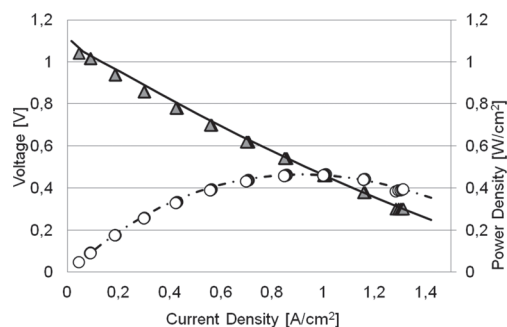
Fig. 2. Voltage [V] and power-current curves for the single mSOFC at temperature 750 [°C] for pure hydrogen: △ - voltage of experiments [12], ○ - power density of experiments [*Howe and Kendall, 2011*], ——-voltage from CFD, — · — - power density from CFD
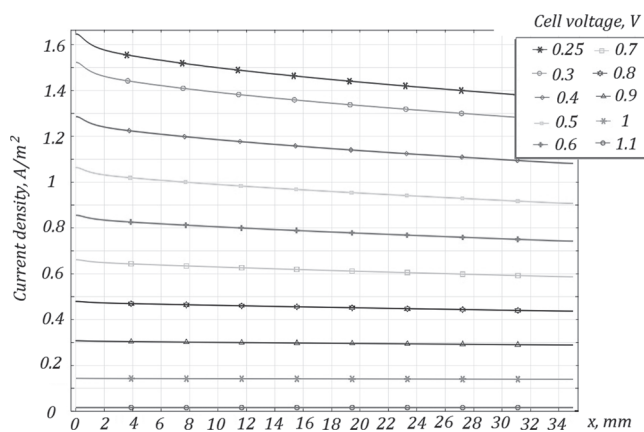

Fig. 3. The anode current distribution along the SOFC length

Conclusions

A simple 2D CFD model of the single microtubular SOFC was established for the purpose of future stack and system simulations. The model took into account coupled processes of hydrodynamics, diffusion, electrochemistry and charge transfer taking place in the mSOFC studied. The temperature and equilibrium potential distributions were assumed to be uniform in the presented numerical case. The estimated mSOFCs performance, i.e. voltage- and power-curves as well as the fuel utilization value were close to those in experiments [*Howe and Kendall, 2011*]. Such conclusions encourage us to continue the presented mSOFC study since accurate predictions of the heat transfer and concentration polarization in the single mSOFC are still a challenging task and require further studies.

LITERATURE

Akhtar N. et al., 2010. Numerical modelling of methane-powered micro-tubular, single-chamber solid oxide fuel cell. *J. of Power Sources,* **195**, 7796–7807. DOI: 10.1016/j.jpowsour.2010.01.084

Akhtar N., 2012. Micro-tubular, single-chamber solid oxide fuel cell (MT–SC-SOFC) stacks: Model development. *Chem. Eng. Res. Des.*, **90**, 814–824. DOI: 10.1016/j.cherd.2011.09.013

Ameri M., Mohammadi R., 2011. Simulation of an atmospheric SOFC and gas turbine hybrid system using Aspen Plus software. *Int. J. Energy Res.*, **37**, 5, 412-425. DOI: 10.1002/er.1941

Amiri S., Hayes R.E., Nandakumar K., Sarka P., 2013. Modelling heat transfer for a tubular micro-solid oxide fuel cell with experimental validation. *J. Power Sources*, **233**, 190–201. DOI: 10.1016/j.jpowsour.2013.01.070

Bistolfi M., Malandrino A., Mancini N., 1996. The use of different modeling approaches and tools to support research activities: an industrial example. *Comp. Chem. Eng.*, **20**, SI487-S1491. DOI: 10.1016/0098-1354(96)00253-0

Costamagna P., Costa P., Antonucci V., 1998. Micro-modeling of solid oxide fuel cell electrodes. *Electrochimica Acta*, **43**, 375-394. DOI: 10.1016/S0013-4686(97)00063-7

Cui D., Cheng M., 2009. Numerical analysis of thermal and electrochemical phenomena for anode supported microtubular SOFC. *AIChE J.*, **55**, 3, 771-782. DOI: 10.1002/aic.11697

COMSOL Multiphysics Version 4.3, Batteries & Fuel Cells Module, User's Guide (04.2013): http://nf.nci.org.au/facilities/software/COMSOL/4.3/doc/pdf/mph/COMSOLMultiphysicsUsersGuide.pdf

Ferguson J.R. Fiard J.M., Herbin R., 1996 Three-dimensional numerical simulation for various geometries of solid oxide fuel cells. *J. Power Sources*, **58**, 2, 109-122. DOI: 10.1016/0378-7753(95)02269-4

García-Camprubí M. Jasak H., Fueyo N., 2011. CFD analysis of cooling effects in H₂-fed solid oxide fuel cells. *J. Power Sources*, **196,** 7290– 7301. DOI: 10.1016/j.jpowsour.2011.04.037

Howe K., Kendall K., 2011a. Transient performance of micro-tubular solid oxide fuel cells and stacks. *ECS Trans.,* **35**, 1, 419-423. DOI: 10.1149/1.3570017

Howe K., Thompson G.J., Kendall K., 2011b. Micro-tubular solid oxide fuel cells and stacks. *J. Power Sources,* 196, 4, 1677–1686. DOI: 10.1016/j.jpowsour.2010.09.043

Hussain M.M. Li X., Dincer I., 2009. A general electrolyte-electrode-assembly model for the performance characteristics of planar anode-supported solid oxide fuel cells. *J. Power Sources,* **189**, 2, 916–928. DOI: 10.1016/j.jpowsour.2008.12.121

Kendall K., 2010. Progress in microtubular solid oxide fuel cells. *Int. J. Appl. Ceram. Technol., 7, nr 1, 1-9*. DOI: 10.1111/j.1744-7402.2008.02350.x

Kulikovsky A.A., 2009. A model for solid oxide fuel cell anode performance. *Electrochimica Acta*, **54**, 26, 6686–6695. DOI: 10.1016/j.electacta.2009.06.054,

Lee S-B., Lim T-H., Song R-H., Shin D-R., Dong S-K., 2008. Development of a 700 W anode-supported micro-tubular solid oxide fuel cell stack for APU applications. *Int. J. Hydrogen Energy*, **33**, 2330 – 2336. DOI: 10.1016/j.ijhydene.2008.02.034

Lee S-B., Hong C-W., 2010. Multi-scale design simulation of a novel intermediate temperature micro solid oxide fuel cell stack system. *Int. J. of Hydrogen Energy*, **35**, 1330-1338. DOI: 10.1016/j.ijhydene.2009.11.095

Lockett M., Simmons M.J.H., Kendall K., 2004. CFD to predict temperature profile for scale up of micro oxide fuel cell stacks. *J. Power Sources*, **131**, 1-2, 243–246. DOI: 10.1016/j.jpowsour.2003.11.082

Nield D. A., Bejan A., 2006. *Convection in porous media*. Springer, New York.

Zeng M. Juang J., Zhang J., Sundén B., 2012. Investigation of thermal radiation effects on solid oxide fuel cell performance by a comprehensive model. *J. Power Sources*, **206**, 185-196. DOI: 10.1016/j.jpowsour.2012.01.130

Zhang W. Croiset E., Douglas P.L., Fowler M.W., Entchew E., 2005. Simulation of a tubular solid oxide fuel cell stack using AspenPlusTM unit operation models. *Energy Conv. Man.*, **46**, 2, 181–196. DOI: 10.1016/j.enconman.2004.03.002